MITLibraries | DSpace@MIT

MIT Open Access Articles

A method for guiding ablation catheters to arrhythmogenic sites using body surface electrocardiographic signals

Massachusetts Institute of Technology

A Method for Guiding Ablation Catheters to Arrhythmogenic Sites Using Body Surface Electrocardiographic Signals

Maya E. Barley*, Antonis A. Armoundas, *Member, IEEE*, and Richard J. Cohen

Abstract—**Treatment of hemodynamically unstable ventricular arrhythmias requires rapid and accurate localization of the reentrant circuit. We have previously described an algorithm that uses the single-equivalent moving dipole model to rapidly identify both the location of cardiac sources from body surface electrocardiographic signals and the location of the ablation catheter tip from current pulses delivered at the tip. However, during catheter ablation, in the presence of sources of systematic error, even if the exit site and catheter tip dipole are superposed in real space, their calculated positions may be separated by as much as 5 mm if their orientations are not exactly matched. In this study, we present a method to compensate for the effect of dipole orientation and examine the method's ability to guide a dipole at a catheter tip to an arrhythmogenic dipole corresponding to the exit site. In computer simulations, we show that the new method enables the user to guide the catheter tip to within 1.5 mm of the arrhythmogenic dipole using a realistic number of movements of the ablation catheter. These results suggest that this method has the potential to greatly facilitate RF ablation procedures, especially in the significant patient population with hemodynamically unstable arrhythmias.**

Index Terms—**Catheter ablation, equivalent moving dipole, ventricular tachycardia (VT).**

I. INTRODUCTION

CARDIOVASCULAR disease is the most prominent cause of morbidity in the developed world. In the USA alone, approximately 465 000 people die each year from heart disease [1]. Many of these deaths are sudden—specific estimates range from 36% to as high as 65% [1], [2]—and presumed to be caused by ventricular tachycardia (VT) and/or fibrillation, for which there are several underlying causes. The majority of patients in the USA experiencing VT have underlying coronary artery disease [3]. The most common etiology of VT in the presence of infarcted tissue is the formation of a reentrant circuit, in which electrical activity circulates rapidly through and around a zone of infarction, creating a self-sustaining cycle of abnormal impulse conduction [4].

While the implantable cardioverter defibrillator (ICD) [5]–[7] is an effective means for terminating the VT after it is initiated, a treatment of VT would be desirable. The current method of choice for the prevention of reentrant VT is RF ablation (RFA) [8], [9]. RFA treatment of arrhythmias involves the guidance of an ablation catheter to the isthmus or the exit site of the reentrant circuit and the administration of high-intensity RF current to the tissue. Therefore, RFA requires both the *accurate localization* of the isthmus or the exit site of the reentrant circuit and the *accurate guidance* of the ablation catheter to that site.

The cardiac excitation pattern at any instant can be conceptualized as a wavefront of electric dipoles. Mathematically, it is not possible to reconstruct the 3-D distribution of electrical sources in the heart from body surface measurements since the solution is not unique [10]. Furthermore, cardiac electrical activity is attenuated, distorted, and smoothed in the torso volume conductor (the medium between the heart and the body surface), and thus, the body surface potential distribution is a distorted image of the cardiac electrical activity [11]. However, in an attempt to understand cardiac electrical activity, numerous models have been developed that represent this instantaneous activity by an equivalent source that may consist of single or multiple dipoles that may be fixed or moving [10]. Several models also exist that reconstruct electrical activity in the epicardium or myocardium from measured surface electrocardiographic potentials [12]–[14]. To overcome the nonuniqueness of the problem, we have chosen to model cardiac electrical activity with a single-equivalent moving dipole (SEMD). This is a simplification of the true cardiac bioelectric activity. Consequently, it is an oversimplified model of cardiac electrical activity when that activity is spatially distributed, and thus, at these times, the inverse problem does not have a unique solution. However, we believe that the SEMD model provides a valid approximation of cardiac electrophysiological events when the heart's electrical activity is spatially well localized, for example, when a wave of depolarization is first emerging from the exit site of a reentrant circuit [15]. In this case, the SEMD solution is represented by a set of six parameters that describe the location and moment of the *single* dipole that best reproduces the potentials at a given set of electrodes at a given time instant [16].

We have previously presented an algorithm that estimates the instantaneous location and moment of the single-equivalent

dipole from multiple-lead body surface ECGs [17]. We shall term this the *inverse solution guidance algorithm* (ISGA). In this algorithm, for a set of instantaneous body surface potentials, the volume of an idealized torso model is searched for the dipole moment and location such that the resultant potentials estimated by the model best replicate the measured body surface potentials. Dipole parameters can then be estimated for each time sample of a single beat of VT to find the trajectory of the single-equivalent dipole over the entire cardiac cycle. From analysis of this trajectory, the dipole whose location best corresponds to the exit site of the reentrant circuit may be selected. We shall term the dipole resulting from activity at the exit site the *arrhythmogenic dipole*. Since the arrhythmogenic dipole is computed from body surface potentials that, in turn, reflect *all* ongoing electrical activity in the heart, the single dipole approximation will only be accurate if no remote electrical activity from the previous VT cardiac cycle is present at the beginning of the next QRS complex. Consequently, in this study, we assume that periods of isoelectricity are present in the VT waveform.

However, RFA requires both the localization of the isthmus or the exit site of the reentrant circuit *and* the guidance of an ablation catheter to this site. Our approach tackles both of these problems, by using the ISGA to also determine the location and orientation of the catheter tip. Specifically, using surface potentials generated by a current dipole between electrodes at the tip of a specially designed ablation catheter, the ISGA may be used to estimate the catheter tip dipole location and orientation. The current between the catheter tip electrodes will be at a frequency well above that of bioelectrical signals (0.1–125 Hz) but below that at which the frequency response of the torso becomes measurably different (>1 kHz); the catheter tip signal may then be separated from the cardiac signal using a bandpass filter. In this way, an ablation catheter tip may be guided to the exit site of the reentrant circuit for the accurate delivery of ablative energy. While the diameter of ablation lesions may vary in diameter from approximately 5 to over 8 mm [18], only the lesion's central core is necrotic and will not heal after the procedure [19]. Therefore, the catheter should ideally be guided within 2–3 mm of the exit site for long-term success of the procedure.

By using an infinite, homogeneous forward model, the ISGA solution may be estimated in real time (a necessity during an ablation procedure). However, this simplification also results in a difference between the real and estimated locations of the SEMD. The effect of ignoring all torso inhomogeneities [20], boundary effects, and inaccuracies in electrode positions introduces systematic error into the estimation; the position of the arrhythmogenic dipole *image* as determined by the ISGA is expected to be displaced from its *true* position by some error vector whose magnitude and direction will be dependent on the specific nature of the nonidealities. Here, we refer to the estimated dipole positions and moments as the dipole *images* to distinguish them from the *real* dipole locations and moments in physical space.

How does this displacement affect our ability to superpose the catheter tip dipole with the arrhythmogenic dipole? Clearly, if the two dipoles are in reality matched in *both* location and orientation, a purely systematic error will distort the estimation of their locations *equally,* and their images will appear perfectly superposed. Simulations conducted by Armoundas *et al.* [15] have shown that in a bounded torso model and in the presence of 0.01 mV Gaussian measurement noise, two superposed and cooriented dipoles will be estimated to lie within 0.4 mm of each other; although noise prevents exact alignment in image space, two cooriented dipoles still appear essentially superposed. However, will the images of two dipoles whose moments are *not* aligned also appear superposed? Studies with numerical simulations of a torso model with realistic geometries and conductivities have implied that if the dipoles are differently oriented, this may significantly affect the accuracy of ISGA [21]. However, the size of this effect has not been quantified. Furthermore, its consequence on the accuracy of catheter *guidance* (rather than stationary source localization) has not been assessed.

Therefore, the purpose of this study is first to analyze the effect of dipole orientation on the ability of the ISGA to colocalize two superposed dipoles in the presence of sources of systematic error. We first show that the original ISGA does not guarantee accurate superposition of two dipoles whose moments are not aligned. We then present a method to compensate for the effect of orientation in the presence of sources of systematic error. This method utilizes a special catheter tip design on which four electrodes are placed at the catheter tip in such configuration in order to produce three orthogonal dipoles. If these dipoles are stimulated consecutively at the same location, they produce three sets of torso surface potentials. Our method weights and sums these surface potentials to produce a set of potentials identical, within the level of measurement noise, and the set of body surface potentials due to the arrhythmogenic dipole, provided that the catheter tip is superposed with the arrhythmogenic dipole. We propose and evaluate three methods to guide the ablation catheter toward the arrhythmogenic dipole to achieve such superposition.

We use computer simulations to test each method's ability to guide a moving catheter tip dipole toward a fixed arrhythmogenic dipole and also evaluate the superposition accuracy of two dipoles in the presence of significant systematic error. Catheter guidance is simulated in both a bounded spherical model and a torso model with realistic geometries and conductivities. This study is expected to provide a significant initial assessment of the ISGA's ability to guide ablation therapy.

II. METHODS

A. Forward Model

Two forward models were used: a bounded, homogeneous, spherical model, and other bounded, inhomogeneous model of a human torso with realistic geometries and conductivities. The first model presented a simple but effective model of systematic error in order to rapidly test and compare guidance methods. The second model allowed a realistic catheter guidance procedure to be simulated, and the superposition accuracy of the catheter tip with a simulated arrhythmogenic source to be estimated.

1) Bounded, Homogeneous, Spherical Model With Inaccurate Electrode Positioning: Simulations were conducted with a homogenous spherical torso model of radius 12.5 cm. A total of 60 electrodes were distributed on the sphere surface in a 12.5 × 12.5 cm square grid of 25 electrodes (interelectrode separation = 3.125 cm), with the other 35 electrodes distributed randomly over the spherical surface. The electrode grid was centered at the point on the torso surface closest to the stationary dipole simulating the arrhythmogenic dipole (we shall continue to refer to it as the arrhythmogenic dipole for consistency). This layout takes into consideration the eventual application of this paper in RFA procedures.

We used the equation derived by Frank [22] to estimate the potentials on the surface of the bounded spherical torso due to a dipole (p_x, p_y, p_z) located along the z-axis at $z = fR (0 \leq f \leq 1;$ R: radius of the sphere)

$$
\varphi^i = \frac{p_z}{4\pi g f R^2} \left[\frac{1 - f^2}{(1 + f^2 - 2f\mu^i)^{3/2}} - 1 \right]
$$
$$
+ \frac{p_x \cos \psi^i + p_y \sin \psi^i}{4\pi g f R^2 \sin \theta^i} \left[\frac{3f - 3f^2\mu^i + f^3 - \mu^i}{(1 + f^2 - 2f\mu^i)^{3/2}} + \mu^i \right]
$$
$$(1)$$

where $\mu^i = \cos(\theta^i)$, and θ^i and ψ^i are the azimuth and latitude angles of the ith surface electrode, respectively, and g is the conductivity of the spherical medium.

Inaccurate electrode positions were generated by adding errors drawn from a Gaussian distribution ($\mu_e = 0, \sigma_e = 0.5$ cm) to each of the x, y, and z coordinates of each correct electrode location. The forward problem utilized the *real* electrode locations and the bounded torso model defined by (1) to simulate measured surface potentials for a given dipole. The ISGA, on the other hand, used the *assumed* electrode locations and the infinite volume conductor estimation defined by (2) in order to estimate the dipole parameters. Finally, we added Gaussian white noise ($\mu_m = 0, \sigma_m = 0.01$ mV) to the measured surface potentials to account for a realistic level of measurement noise.

2) Bounded Element Method for Realistic Human Torso Model: A previously described boundary element method (BEM) was used to forward model the surface potentials due to a dipole of known position and strength inside the heart of a realistic human torso model [21]. The torso model and electrode positions are shown in Fig. 1. The model is composed of bounded, homogeneous, and isotropic compartments, whose surfaces are discretized into triangles. The torso model used in this study consisted of realistically shaped compartments (whose geometries were generated from MRI images), representing the torso, heart, and lungs. The boundary surfaces of the piecewise homogeneous torso, heart, and lung compartments were formed by triangular meshes of 1280, 380, and 1120 triangles, respectively. As in the study by Armoundas *et al.*, the conductivities assigned to the torso, lungs, and heart (including the ventricular chambers) were 0.2, 0.45, and 0.04 S/m, respectively. The body surface potential distribution due to a dipole inside the heart was estimated at the 64 indicated electrode positions.
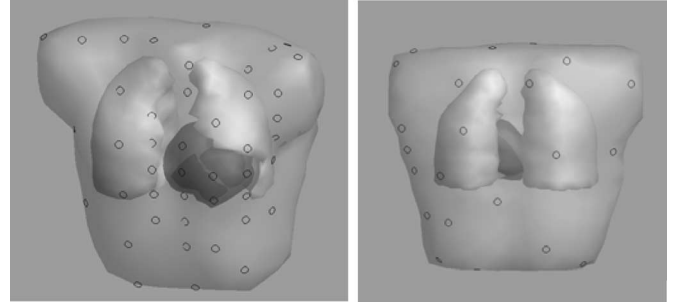

Fig. 1. 3-D volume conductor model of the human torso used to forward-model the surface potentials of a dipole inside the heart. The bounded element model of the torso consisted of realistically shaped organ compartments (whose geometries had been generated from MRI images), representing the lungs, heart and torso surface. The positions of the surface electrode are also shown.

B. Inverse Solution Guidance Algorithm

In the ISGA, for a given dipole location, magnitude, and orientation, the estimated forward potential at the ith body surface electrode φ_f^i due to a single dipole is estimated using an infinite volume conductor model [15]

$$
\varphi_f^i = \frac{\mathbf{p}(\mathbf{r} - \mathbf{r}_i')}{4\pi g |\mathbf{r} - \mathbf{r}_i'|^3}
\tag{2}
$$

where $\mathbf{r}_i'$ represents the ith electrode location, $\mathbf{r}$ the dipole location, $\mathbf{p}$ the dipole moment, and g the conductivity of the volume conductor. An objective function χ^2 describes how well the dipole reproduces the measured voltages

$$
\chi^2 = \sum_{i=1}^{I} \left(\frac{\varphi_f^i - \varphi_m^i}{\sigma_m^i} \right)^2
\tag{3}
$$

where φ_m^i is the measured potential at the ith electrode, σ_m^i is the standard deviation of the measurement noise in lead i, and I is the number of electrodes ($I = 60$).

In the application of the ISGA, voltages are measured at 60 electrodes on the volume conductor surface, and a *brute-force* search method is used to find the SEMD parameters that best fit a time sample of the measured data. A brute-force method is used instead of a simplex search because of the presence of local objective-function minima in the highly nonlinear parameter space. By using a brute-force search, the algorithm becomes more computationally demanding. However, the algorithm is forced to return a solution that represents the *absolute* minimum of the χ^2 objective function. The search process commences with discretization of the volume into cubic volumes 1.5 cm on a side. A dipole is simulated to lie at the center of each cube, and its moment is optimized, using the relationship defined by (2) to most closely reproduce the measured potentials (this optimization strategy has previously been termed *three-plus-three* parameter optimization as the three locations are optimized independently from the three moment parameters [16]). The three dipoles whose locations and moments yield the *three* lowest χ^2-values at 1.5 cm resolution are then selected. Next, the three cubes containing these dipoles *and* their neighboring cubes are discretized into smaller cubes, and the χ^2 minimization procedure is repeated to find the three optimal

dipoles at this higher resolution. This process is iterated until the cube dimension is less than 1 mm to a side. At this resolution, the dipole whose estimated body surface potentials best reproduce the measured voltages is selected as the SEMD for that time sample.

The cubes containing the lowest χ^2-values at each resolution may not be contiguous as a result of the presence of local minima in the objective function landscape; by examining multiple regions in the volume conductor at a higher resolution, we continue the search in the region of objective function space that contains only the absolute minimum. We have previously verified in simulations in a bounded spherical model that by using this search method, we prevent the algorithm from returning a solution that represents only a local minimum of the χ^2 objective function in parameter space, and instead, force it to find the absolute minimum.

C. Assessment of Significance of Dipole Orientation

It has been shown that the error between true and estimated dipole positions in a bounded sphere is small enough that an ablation catheter may be *guided* toward the site of the arrhythmogenic dipole using the ISGA [15]. However, if the ISGA is to be used to accurately superpose the ablation catheter with the arrhythmogenic dipole, a parameter of great importance is the distance between two dipole images whose real dipole locations are superposed in space but whose real dipole moments are not aligned. This parameter reflects the ability of the algorithm to detect the final superposition of the ablation catheter tip with the arrhythmogenic dipole.

To this end, simulations were performed using the previously described spherical model to investigate the effect of dipole orientation in the presence of boundary effects and inaccurate electrode positioning on the location of the dipole image solution. At consecutive locations along the z-axis, we placed a dipole of constant magnitude (sufficient to generate maximum surface potentials on the order of 0.1 mV). At each dipole location, we conducted 100 simulations using random dipole orientations, and recorded the 100 dipole image positions estimated by the ISGA. For each set of 100 dipole image positions, we calculated the mean location of the dipole images. We then computed the dipole image *dispersion* (the standard deviation of the absolute distance of each dipole image location from the mean dipole image location). This quantifies how widely the dipole images are scattered in 3-D image space. This reflects how accurately the ISGA will detect the superposition of two dipoles whose real locations are superposed but whose orientations are different. We wish to assess the size of the dispersion of the *real* dipole given superposed dipole *images*; therefore, we assume that the dispersion in image space is a good estimate of the dispersion in real space. Since an ablation accuracy of 2–3 mm is ideal, we must consider using an improved algorithm to compensate for the effect of dipole orientation if the magnitude of the dipole image dispersion indicates that this level of accuracy is not consistently achievable.

D. Method to Compensate for Effect of Orientation

1) Multiple Catheter Tip Electrodes to Mimic Dipole Orientation: To compensate for the effect of dipole orientation, we propose a special catheter with a single positive electrode at its tip and three negative electrodes arrayed a few millimeters further down the shaft, such that three independent dipoles of equal magnitude can be generated consecutively from the same focus on the catheter tip. The three resulting body surface potentials at each electrode i due to the three dipoles $\varphi i = [\varphi_1^i, \varphi_2^i, \varphi_3^i]^T$, where $i \in \{1, 2, \ldots, I\}$, may be weighted and summed to produce a voltage φ_λ^i, using a weighting vector $\boldsymbol{\lambda} = [\lambda_1, \lambda_2, \lambda_3]$

$$\varphi_\lambda^i = \boldsymbol{\lambda} \cdot \boldsymbol{\varphi}^i. \tag{4}$$

Due to the linear relationship between dipole moment and body surface potentials, φ_λ^i is the set of potentials that would have resulted if a dipole of orientation $\mathbf{p}_\lambda = \boldsymbol{\lambda} \cdot P$ (where P is a 3×3 matrix in which each row represents one of the three dipole moments corresponding to the three independent catheter tip dipoles) were generated at the catheter tip. By recording the three sets of body surface potentials generated consecutively by three independent dipoles at the same catheter tip location, and then choosing a single $\boldsymbol{\lambda}$ to be used for all I electrodes, we can reproduce the set of potentials that would have resulted from a dipole of orientation $\mathbf{p}_\lambda$ placed at the catheter tip. This allows us to simulate the surface potentials of a dipole of any moment at the catheter tip, regardless of physical tip orientation.

Let $\mathbf{p}_a$ be the moment vector of the arrhythmogenic dipole image and $\boldsymbol{\varphi}_a^i = [\varphi_a^1, \varphi_a^2, \ldots, \varphi_a^I]$ the resultant instantaneous surface potentials due to the arrhythmogenic dipole. *If the catheter tip is perfectly superposed with the arrhythmogenic dipole, a unique weight $\tilde{\lambda}$ can be found to create a $\varphi \tilde{\lambda}^i = [\varphi \tilde{\lambda}^1, \varphi \tilde{\lambda}^2, \ldots, \varphi \tilde{\lambda}^I]$ that is indistinguishable from $\boldsymbol{\varphi}_a$ (to within the level of measurement noise).* If a brute-force search is applied to $\varphi \tilde{\lambda}$, the SEMD solution will be equivalent to that for $\boldsymbol{\varphi}_a$, correctly indicating dipole superposition regardless of catheter tip orientation.

2) Estimation of $\tilde{\lambda}$: We define the error E_λ as the sum over all body surface electrodes of the squared normalized difference between the potentials recorded at each surface electrode due to the arrhythmogenic dipole φ_a^i and a weighted sum, $\varphi_\lambda^i = \boldsymbol{\lambda} \cdot \boldsymbol{\varphi}^i$, of the potentials recorded at each electrode from the dipoles at the ablation catheter tip

$$E_\lambda = \sum_{i=1}^{I} \left(\frac{\varphi_a^i - \varphi_\lambda^i}{\sigma_m^i} \right)^2. \tag{5}$$

For a set of three body surface potentials corresponding to three different dipoles generated at the catheter tip, expressed in the matrix $\boldsymbol{\Phi} = [\boldsymbol{\varphi}_1, \boldsymbol{\varphi}_2, \boldsymbol{\varphi}_3]^T$, where $\boldsymbol{\varphi}_j = [\varphi_j^1, \varphi_j^2, \ldots, \varphi_j^I]^T$ and $j \in \{1, 2, 3\}$, we find the $\boldsymbol{\lambda}$ that minimizes E_λ. $\tilde{\boldsymbol{\lambda}}$ is the value of $\boldsymbol{\lambda}$ that minimizes E_λ. $\varphi \tilde{\lambda}$ is then defined as

$$\varphi_{\tilde{\lambda}} = \tilde{\boldsymbol{\lambda}} \cdot \Phi. \tag{6}$$

If the catheter tip is superposed with the real location of the arrhythmogenic dipole, $\varphi \tilde{\lambda}$ will be equivalent to φ_a, the

body surface potentials due to the arrhythmogenic dipole. If the catheter tip and arrhythmogenic dipole are *not* superposed, it will be impossible to find a $\tilde{\boldsymbol{\lambda}}$ for which $\boldsymbol{\varphi}\tilde{\boldsymbol{\lambda}}$ is equivalent to $\boldsymbol{\varphi}_a$. Instead, $\boldsymbol{\varphi}\tilde{\boldsymbol{\lambda}}$ will be the closest approximation $\boldsymbol{\varphi}_a$ given the set of three body surface potentials $\boldsymbol{\Phi}$. Since this method compares the measured surface potentials from the cardiac and catheter tip dipoles, we shall term it the *cardiac signal comparison* (CSC) method.

3) Achieving Superposition: We explored two ways in which to perform the brute-force search to find the best-fit SEMD approximation to $\boldsymbol{\varphi}\tilde{\boldsymbol{\lambda}}$: method I, in which both the moment and the location of the SEMD are chosen by the three-plus-three parameter optimization outlined in Section II-B [16], and method II, in which the SEMD is restricted to a dipole of moment $\mathbf{p}_a$ regardless of catheter tip position, and therefore, only the dipole location is optimized.

The homogenous, unbounded model used in the ISGA may lack the complexity to accurately fit two sets of surface potentials from slightly different locations due to the applied approximations. Therefore, at catheter tip positions close to the arrhythmogenic dipole, method I may falsely indicate superposition of the catheter tip with the arrhythmogenic dipole. The parameter

$$\chi_a^2 = \sum_{i=1}^{I} \left(\frac{\varphi_f^i - \varphi_a^i}{\sigma_m^i} \right)^2 \tag{7}$$

provides insight into the degree of systematic error at the arrhythmogenic dipole location since its magnitude is proportional to the dissimilarity between the infinite, homogenous model and the bounded, nonideal torso. The higher the χ_a^2 value, the less accurate the SEMD estimation and the greater the possibility that method I will falsely indicate superposition. The greater the distance that the catheter tip is from the arrhythmogenic dipole, the more likely it is that method I will falsely indicate superposition.

This is not a concern if the dipole moment is fixed during the brute-force search (method II) so that the solution has the same orientation as the arrhythmogenic dipole image at all times. Empirically, we find that this method indicates superposition only if the dipole images correspond in both location and moment. However, searching for a dipole of orientation $\mathbf{p}_a$ when the catheter is far from the arrhythmogenic dipole may result in the estimated image location of the catheter tip being significantly displaced from its real location. As the catheter and arrhythmogenic dipole images are brought closer, the image position estimation will become more accurate. For more discussion on the dipole image location estimation using method II, please see the Appendix.

Methods I and II appear to work best in complementary regimes, and we hypothesize that the ideal algorithm is a robust combination that most efficiently converges on the correct solution.

4) Combined CSC Method: The combined approach allows the methods to work in the regimes in which they operate most effectively: at locations further from the arrhythmogenic dipole, we employ method I, while at locations close to the arrhyth-

mogenic dipole, method II should be the principal component. Furthermore, the transition between these two methods must be smooth.

The distance at which method I errors might be more pronounced depends greatly on the nature of the systematic error and the location of the arrhythmogenic dipole. If the measured potentials of the arrhythmogenic dipole $\boldsymbol{\varphi}_a$ are more similar to the weighted-and-summed catheter dipole potentials $\boldsymbol{\varphi}\tilde{\boldsymbol{\lambda}}$ than the forward-modeled potentials of the arrhythmogenic dipole image $\boldsymbol{\varphi}_f$, then the catheter tip location could be erroneously identified to be the same as that of the arrhythmogenic dipole image. Therefore, we base our approach on a comparison of χ_a^2 with a parameter that measures the similarity of $\boldsymbol{\varphi}_a$ and $\boldsymbol{\varphi}\tilde{\boldsymbol{\lambda}}$. This is the minimum value of E

$$E_{\tilde{\boldsymbol{\lambda}}} = \sum_{i=1}^{I} \left(\frac{\varphi_a^i - \varphi_{\tilde{\boldsymbol{\lambda}}}^i}{\sigma_m^i} \right)^2. \tag{8}$$

If $E_{\tilde{\boldsymbol{\lambda}}}$ is less than χ_a^2, $\boldsymbol{\varphi}_a$ is more similar to $\boldsymbol{\varphi}\tilde{\boldsymbol{\lambda}}$ than $\boldsymbol{\varphi}_f$; the homogenous, unbounded model may not adequately discriminate between $\boldsymbol{\varphi}\tilde{\boldsymbol{\lambda}}$ and $\boldsymbol{\varphi}_a$, and may not accurately estimate the distance between the cardiac and catheter dipoles. Hence, method I might fail. The smaller the ratio of $E_{\tilde{\boldsymbol{\lambda}}}$ to χ_a^2, the more likely this is to happen. Therefore, for $E_{\tilde{\boldsymbol{\lambda}}} < \chi_a^2$, method II is introduced to a degree determined by the ratio of $E_{\tilde{\boldsymbol{\lambda}}}$ to χ_a^2. A weighting factor $W(E_{\tilde{\boldsymbol{\lambda}}}/\chi_a^2)$, is used to weight the contributions from methods I and II to the final solution when $E_{\tilde{\boldsymbol{\lambda}}} < \chi_a^2$. When $E_{\tilde{\boldsymbol{\lambda}}} \geq \chi_a^2$, method I is used.

When $E_{\tilde{\boldsymbol{\lambda}}}$ is only slightly less than χ_a^2, the distortion in the method II solution might be high since the catheter tip and arrhythmogenic dipole might be a significant distance apart. Therefore, W should preferentially weight the solution from method I, while providing some small input from method II. As the ratio of $E_{\tilde{\boldsymbol{\lambda}}}$ to χ_a^2 decreases, the solutions from methods I and II will converge, and the latter should be introduced to a greater extent. The transition of emphasis from method I to method II must be sufficiently gradual so that the distance and directionality of movement are realistic.

We empirically chose a function $W(E_{\tilde{\boldsymbol{\lambda}}}/\chi_a^2)$ that fits these criteria

$$W\left(\frac{E_{\tilde{\boldsymbol{\lambda}}}}{\chi_a^2}\right) = \left(\frac{E_{\tilde{\boldsymbol{\lambda}}}}{\chi_a^2}\right)^{\gamma} \tag{9}$$

where γ is a constant whose value we optimized (using data presented in this paper) at 0.415. The dipole image locations estimated by CSC method I ($\mathbf{r}_I$) and method II ($\mathbf{r}_{II}$) are weighted to produce a new dipole image location $\mathbf{r}_{co}$

$$\mathbf{r}_{co} = W \cdot \mathbf{r}_I + (1 - W) \cdot \mathbf{r}_{II}. \tag{10}$$

A summary flowchart of the combined CSC method is shown in Fig. 2.

E. Simulations to Compare Method Guidance Capabilities

The original ISGA, in which only one catheter tip dipole is used to estimate the location of the catheter tip, was compared with the three new methods developed in this paper that utilize
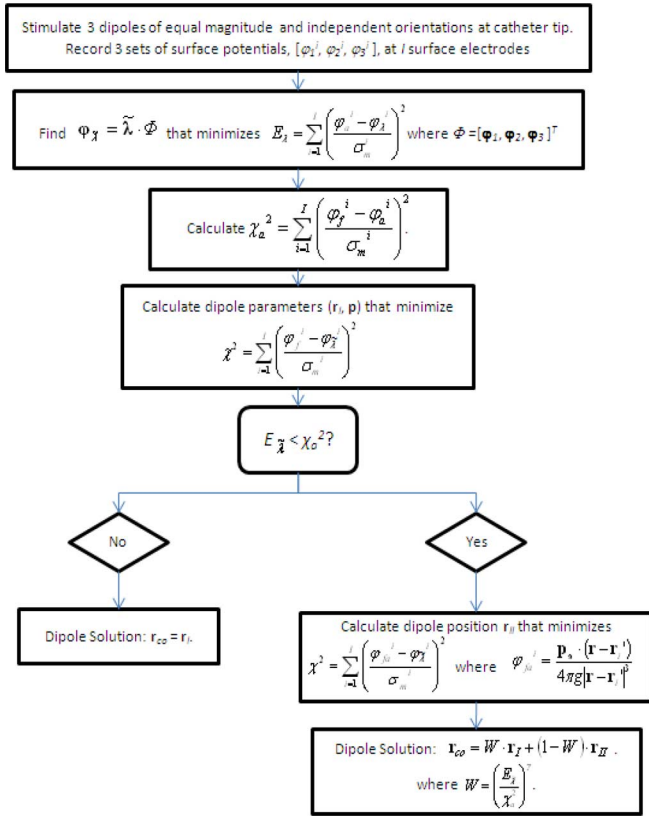
Fig. 2.   Flowchart summarizing the combined CSC method.

multiple catheter tip dipoles. All four methods were tested in simulations conducted in the spherical model described previously. The bounded forward problem is described by (1) for a dipole placed along the z-axis of the sphere. However, rotation of the axes allows the boundary model to be used for dipole locations located anywhere within the spherical torso.

In our simulations, the locations of the arrhythmogenic and catheter tip dipoles were restricted to a bounded "heart volume" within the sphere. The heart was modeled as a sphere of radius 4.5 cm, centered 8 cm from the sphere center. Therefore, the surface of the heart touched the spherical surface at a single point (since boundary conditions become more severe closer to the volume conductor surface, this presented a challenging simulation environment). The electrode grid was centered over the heart volume. The dipole magnitudes used were as described previously. The bounded forward model was used to simulate the potentials at the surface electrodes. As before, the inverse problem was then solved using the inaccurate electrode positions.

The proposed advantage of methods I, II, and the combined method over the original ISGA is their ability to *superpose* two dipoles with greater accuracy. To compare the superposition accuracies of the four methods, the catheter tip was steered toward the arrhythmogenic dipole using *only* the positions of the dipole images estimated by one of the methods, as would be seen on a user interface by the cardiologist. First, the arrhythmogenic dipole and catheter tip were placed at randomly chosen locations within the heart compartment. The arrhythmogenic dipole moment was randomly selected. The catheter tip orientation was

also randomly selected; the fixed configuration of three independent catheter tip dipoles was rotated to correspond to this orientation. The arrhythmogenic dipole image location $\mathbf{r}_a$ was estimated using the original ISGA, while the catheter dipole image location $\mathbf{r}_c$ was estimated using one of the four methods. If the ISGA was used to find $\mathbf{r}_c$, the body surface potentials resulting from only *one* of the three independent dipoles at the catheter tip was used in the estimation. The estimated locations of both the arrhythmogenic dipole and catheter tip were displayed on a 3-D user interface.

Next, the interimage distance vector $\mathbf{d} = \mathbf{r}_a - \mathbf{r}_c$ was calculated. The catheter tip was subsequently moved a fraction α of $|\mathbf{d}|$ along the direction of $\mathbf{d}$ in *real* space, its new image location estimated using method I, and the new interimage distance vector found. This process was repeated until the distance between the catheter tip and arrhythmogenic dipole images as displayed on the user interface was <0.5 mm (this was deemed image superposition). If the images could not be superposed within 200 iterations, the simulation was considered nonconvergent. However, if superposition was achieved, the simulation was stopped. The number of catheter movements required to reach the final catheter tip location was noted. This was repeated two more times for the same arrhythmogenic dipole location, initial catheter tip location, and fraction α of the interimage distance, first using only method II for guidance and then using only the combined method. At no point in the simulation was knowledge of the real locations used.

The guidance capabilities of the three methods and the original ISGA for a fixed value of α were simulated using 100 different randomly chosen arrhythmogenic dipole and initial catheter tip locations. Last, this process was conducted for values of α ranging from one-eighth of the interimage distance to the full value of $|\mathbf{d}|$.

While the advantage of the three new methods over the original ISGA is in the accuracy of the *superposition* of the catheter tip with the arrhythmogenic dipole, we are also interested in the ease with which each method can *guide* the catheter tip toward its target. One measure of this is the number of catheter movements required to achieve dipole superposition in image space, as described earlier. Another measure is the similarity of the distances from the catheter dipole to the arrhythmogenic dipole in real and image spaces, for different distances of the catheter from the arrhythmogenic dipole. To quantify the similarity, the absolute distance of the catheter tip from the arrhythmogenic dipole was compared in image space (i_d) and real space (r_d) for 1000 relative positions of the catheter tip and arrhythmogenic dipole. For each of the four guidance methods, the real space versus image space data were fitted using a least-squares first-order polynomial to establish the relationship between i_d and r_d, and the Euclidean norm of the residuals was calculated (to quantify the degree of scattering of the data).

F. Guidance Simulations in Realistic Torso Model

The guidance capabilities of the combined method and the original ISGA were then compared in the 3-D volume conductor model of the torso with realistic geometries and conductivities.

The arrhythmogenic dipole location was restricted to the endocardial surface, while the catheter tip location was restricted to the same ventricular chamber as the arrhythmogenic dipole. For 50 trials in each of the ventricles, and for each of the two methods, the catheter tip was guided from a randomly chosen initial position toward a randomly chosen arrhythmogenic dipole location. In all cases, the catheter was moved in real space by two-thirds of the interimage distance vector **d**. If image convergence was not achieved within 200 catheter movements, the trial was considered nonconvergent. If image convergence was achieved, the end-point accuracy and the number of catheter movements were noted. For catheter tip and arrhythmogenic dipole positions across all 100 guidance trials, the absolute distance of the catheter tip from the arrhythmogenic dipole was compared in image space (i_d) and real space (r_d). The real space versus image space data were fitted using a least-squares first-order polynomial to establish the relationship between i_d and r_d.

G. Statistical Analysis

The end-point accuracy and number of steps taken were found to follow log-normal distributions. Their results are reported as population mean $\pm$ population standard deviation. Significant differences in these variables were assessed using a two-sided t-test carried out on the log of the data. Statistical significance was assessed at the 0.05 level.

The statistical significance of the differences between the methods' rates of image convergence was assessed by conducting a Wilcoxon signed-rank test on the binary data. Statistical significance was assessed at the 0.05 level.

III. RESULTS

A. Bounded Spherical Model Results

The magnitude of the dipole image dispersion (the standard deviation of the absolute distance between each estimated dipole image and the mean dipole image position) indicates that the images of two perfectly superposed yet differently oriented dipoles may be more than 5 mm apart in the presence of sources of systematic error. This error is greater than the accepted 2–3 mm accuracy required for catheter ablation. Therefore, the need for an improved algorithm that will compensate for the effect of dipole orientation is apparent.

The guidance accuracy of the original ISGA, in which only one catheter tip dipole is used to estimate the location of the catheter tip, was then compared with that of the three new methods developed in this study, which utilize multiple catheter tip dipoles. The first parameter of interest in the comparison of the four methods was the percent image convergence (the percentage of simulations for which the two dipole images, corresponding to the arrhythmogenic dipole and the catheter tip dipole, converged). We found image convergence of between 98% and 99% for all methods, over all step sizes. The difference between algorithms's results was not statistically significantly different.

The number of catheter movements required for the dipole images corresponding to the catheter tip and arrhythmogenic
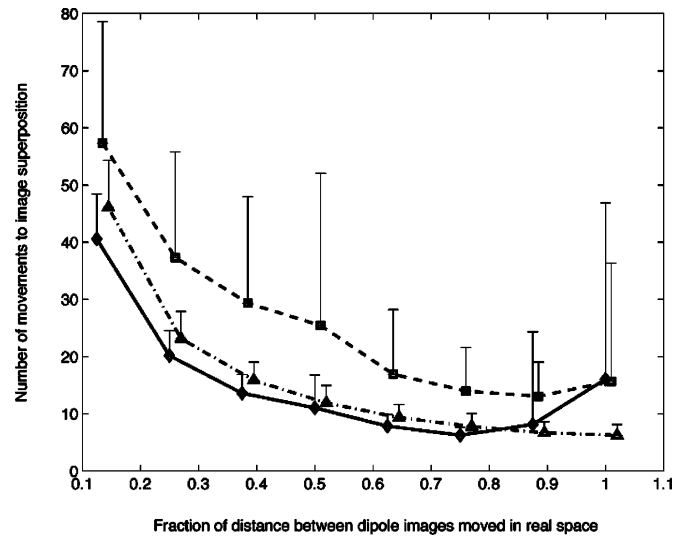

Fig. 3. Mean and standard deviation of the number of catheter movements made to superpose the dipole image corresponding to the catheter tip with the dipole image corresponding to the arrhythmogenic dipole versus α, the fraction of the distance between the two images moved in real space by the catheter tip. Results are shown for when the catheter is guided using method I (*solid line, heptagons*), method II (*dashed line, squares*), and the combined method (*dashed-dotted line, triangle*) in 100 simulations.

dipoles to converge is also important for determining the efficiency of a guiding method. Fig. 3 displays the mean and standard deviation of the number of catheter tip movements required to achieve superposition of the two dipole images, given an end-point accuracy of less than 1.5 mm. We observe that the results of method I and the combined method are substantially lower than that of method II ($p < 0.005$). Special mention must be made of the results for $\alpha = 1$ when the catheter tip is moved at each step by the entire interimage vector. These data provide insight into the ability of each method to correctly represent the relative positions of the real arrhythmogenic dipole and catheter tip. If the representation was exact, the number of steps required to reach the final catheter position would be one. *The combined method appears to offer the best representation of the three methods since it requires the minimum number of steps.*

Last, the distance of the catheter tip from the arrhythmogenic dipole in image space (i_d) and real space (r_d) was compared for 1000 positions of the catheter tip as it moves toward the arrhythmogenic dipole in the spherical homogeneous torso model, using each of the four guiding methods. The least squares best-fit linear relationships between r_d and i_d for method I and the combined method have first-order coefficients of 0.957 and 0.952, respectively. Ideally, the distances in real and image spaces would be equal, resulting in a best-fit line of gradient one. Therefore, these results indicate that distances in image space correspond closely to distances in real space for method I and the combined method. On the other hand, the first-order coefficients of the r_d versus i_d relationship for method II and the original ISGA are 1.379 and 0.817, respectively, reflecting poor correspondence of distances in real and image spaces.

The combined method, therefore, appears to be the best overall guidance method of the three novel methods proposed since it

has both an excellent correspondence between distances in real and image spaces and requires the minimum number of steps for $\alpha = 1$. Therefore, in simulations of catheter guidance in a torso model with realistic geometries and conductivities, only the guidance abilities of the combined method were compared with those of the original ISGA.

B. Guidance Results in Realistic Human Torso Model

1) Dipole Convergence: The guidance accuracy of the original ISGA was compared with that of the combined method. The percent image convergence was 100% in the left ventricle and 96% in the right ventricle, for both methods. In the left ventricle, the end-point accuracy of the combined method was 0.76 ± 0.26 mm, compared with 16.9 ± 8.2 mm for the original ISGA. In the right ventricle, the end-point accuracy of the combined method was 0.80 ± 0.33 mm, and 14.99 ± 5.23 mm for the original ISGA. The combined method thus demonstrates submillimeters accuracy in this model, and a greater-than-one-order-of-magnitude improvement over the original method. It should be noted that the inferior results obtained using the original ISGA were not a consequence of local minima in the objective function space. We ascertained that the absolute minimum of the objective function was found in every case; this was achieved, inspite of the nonlinear parameter space, by using the computationally demanding brute-force search method.

2) Number of Catheter Movements to Achieve Image Convergence: The number of catheter movements required for image convergence in the left and right ventricles was 11.12 ± 1.88 and 8.60 ± 2.14 for the combined method, and 8.60 ± 1.65 and 10.23 ± 2.25 for the original ISGA. These results indicate that the combined method is a highly efficient guidance method, and does not require a greater number of catheter movements than the original algorithm.

3) Comparison of Distances in Image and Real Spaces: Fig. 4(a) and (b) compares the distance of the catheter tip from the arrhythmogenic dipole in image space (i_d) and real space (r_d) for n positions of the catheter tip as it moves toward the arrhythmogenic dipole in the anatomical torso model, using the original ISGA ($n = 791$) and the combined method ($n = 1047$), respectively. In each figure, the solid line depicts the least squares first-order polynomial fit of r_d versus i_d. The polynomial function is also shown. As before, the distances in real and image spaces would ideally be equal, resulting in a best-fit line of gradient one. As illustrated, the polynomial fitted to the combined method data has a gradient of 0.91. This indicates that distances in image space using the combined method correspond closely to distances in real space in the realistic torso model used. However, in the case of the original ISGA, image space is highly distorted by the effect of dipole orientation; this distortion is reflected in the nonlinear relationship between r_d and i_d at smaller distances of the catheter tip from the arrhythmogenic dipole, and the wide distribution of data points around the best-fit line. Furthermore, the correlation coefficient of the combined method data is 0.98, compared with 0.77 for the original ISGA. This indicates a much tighter relationship between real and image spaces for the new guidance algorithm.
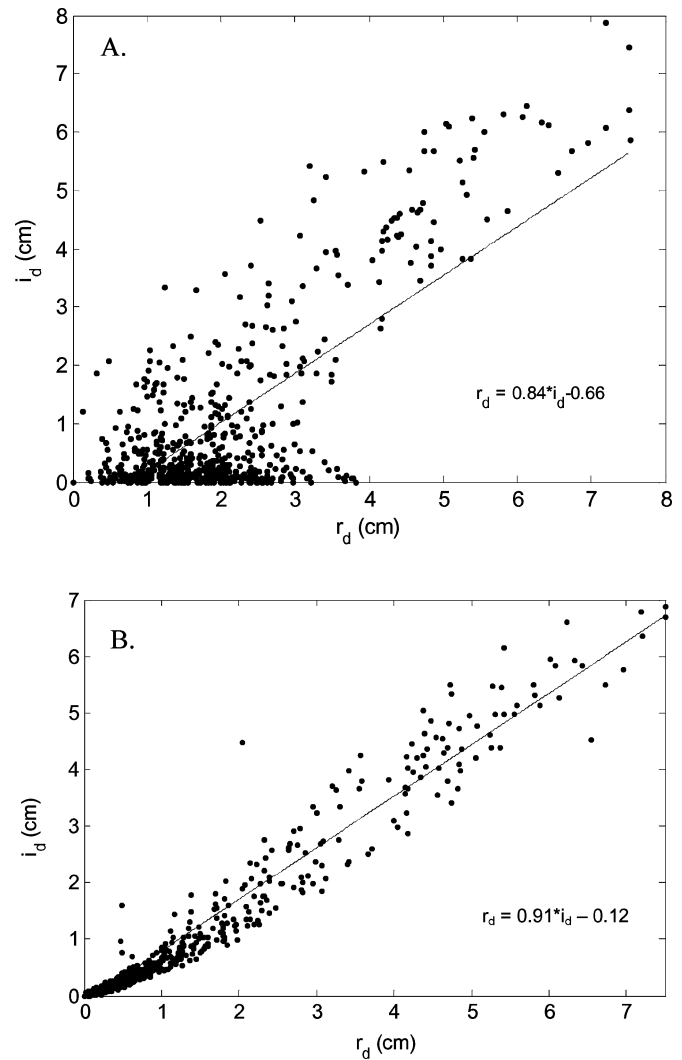

Fig. 4. Distance in the anatomical torso model of the catheter tip dipole from the arrhythmogenic dipole in real space versus the distance between the same two dipoles in image space, for n positions of the catheter tip as it is moved toward the arrhythmogenic dipole. (a) Original ISGA ($n = 791$). (b) Combined method ($n = 1047$).

IV. DISCUSSION

RFA is an important treatment modality for ventricular tachycardia. It requires the accurate guidance of an ablation catheter to the arrhythmogenic origin and the delivery of high-intensity RF current to disrupt the arrhythmogenic pathway. Accurate and speedy guidance of the ablation catheter to the arrhythmogenic site is of prime importance. We have developed an ISGA that may be used to calculate the location of the exit site of a reentrant circuit from noninvasive, multiple-lead body surface ECGs [15], [16], [23].

However, if a current dipole is generated between electrodes at the tip of a specially designed ablation catheter, the ISGA may also be used to estimate the catheter tip location. Therefore this algorithm may be used to guide the ablation catheter tip toward the exit site of the reentrant circuit. In this paper, we explore the effect of dipole orientation in the presence of sources of systematic error (such as boundary effects or inhomogeneities)

on the location estimated by the ISGA described previously [15], [16], [23].

We have developed a specialized catheter design and an algorithm (the CSC method) to compensate for the effect of dipole orientation. We evaluated three methods that we compared with the original inverse registration method in computer simulations. The new methods estimate the catheter location from body surface signals produced by *three* independent dipoles generated between four electrodes at the catheter tip. In contrast, the original inverse registration method estimates the location of the catheter tip from body surface signals produced by only *one* catheter tip dipole.

The combined method is the most consistently accurate of the four methods, with an accuracy of less than 1.5 mm in the model torso. Its accuracy is clearly superior to that of the original inverse algorithm that does not compensate for dipole orientation. Furthermore, the combined method achieves greater accuracies than methods I and II since it uses these two methods in their optimal regimes and minimizes their disadvantages. In addition, we examined the ease with which the catheter tip dipole could be guided to the location of the arrhythmogenic dipole using each method. The number of steps required by method I and the combined method to achieve superposition in image space, and a superposition accuracy of less than 1.5 mm was less than 30 for $0.375 < \alpha < 0.875$. These results suggest that the combined method and method I are both excellent guidance algorithms for directing a catheter tip toward an arrhythmogenic dipole and achieving superposition. Given the greater number of outliers indicating false superposition using method I, the combined method is the preferred option.

Simulations in a torso model with realistic geometries and conductivities indicate that the combined method is both a highly accurate ($<$1.5 mm) and efficient ($<$15 movements) approach for guiding a catheter tip to the site of an arrhythmogenic dipole in the model. Since the core of an ablation lesion is 2–3 mm in diameter, the accuracy of the combined method is suitable for ablation. Furthermore, distances in image space were found to correspond closely to distances in real space using this new method. This agreement between real and image space distances translates into superior hand–eye coordination of catheter tip movements, and consequently, greater ease of use of the guidance method.

The data presented in this study indicate that the combined CSC method overcomes the adverse effect of dipole orientation in the presence of constant systematic error on the ability of the ISGA to guide an ablation catheter tip to the site of an arrhythmogenic dipole. However, the torso model used in this study has several limitations. First, the torso model does not include electrical anisotropies (predominantly from heart and skeletal muscle). Since anisotropies would significantly distort the relationship between real and image spaces, they may have a large effect on the efficiency with which the catheter is guided to its target. In addition, inaccurate electrode positioning, likely in a human or an animal model and which would add an additional source of systematic error, was not taken into account in the torso model simulations.

A further limitation of the static torso model is the lack of natural variation in sources of systematic error. Breathing causes a sub-1-Hz variation in the distribution of torso inhomogeneities and electrode positions. The beating of the heart also causes a change in the tissue distribution around the catheter tip and arrhythmogenic dipole images. In a clinical setting, measures (such as image-gating at end-diastole and breath-holding using a respitrace for guidance) would be taken to reduce changes in systematic error.

In summary, the combined method presented here allows the accurate guidance of an ablation catheter tip to the site of origin of a ventricular arrhythmia in a model torso. Given that the current RFA mapping procedure is generally limited to patients who are hemodynamically stable during VT, the algorithm we have developed here may allow RFA treatment to be administered not only more accurately, but also to a much wider segment of the population affected by VT.

APPENDIX

DIPOLE LOCATION ESTIMATION USING METHOD II

Although $\varphi\tilde{\lambda}$ contains significant information about the location of the catheter tip, it is not always equivalent to the set of body surface potentials φ_{ca} that would be recorded if a dipole of orientation $\mathbf{p}_a$ were placed at the catheter tip. $\varphi\tilde{\lambda}$ and φ_{ca} are only identical in the case that the catheter tip and arrhythmogenic dipole are exactly superposed. At all other locations, $\varphi\tilde{\lambda}$ is skewed toward φ_a since the estimation of $\tilde{\lambda}$ attempts to minimize the difference between these two vectors. Furthermore, it is evident that the degree of this skew is dependent on the distance between the catheter tip and the arrhythmogenic dipole; the greater the distance, the less the $\varphi\tilde{\lambda}$ will resemble φ_{ca}. Since $\varphi\tilde{\lambda}$ is not identical to φ_{ca}, the location found by the brute-force method will be displaced from the actual location of the catheter tip; the further the catheter tip away from the arrhythmogenic dipole, the greater is this displacement. If the catheter tip is aligned with the arrhythmogenic dipole: 1) $\varphi\tilde{\lambda} = \varphi_{ca} = \varphi_a$ and 2) both methods correctly indicate superposition with moment $\mathbf{p}_a$. However, at all other locations, the brute-force search is not likely to yield a dipole of moment $\mathbf{p}_a$.

REFERENCES

[1] T. Thom, N. Haase, W. Rosamond, V. J. Howard, J. Rumsfeld, T. Manolio, Z. J. Zheng, K. Flegal, C. O'Donnell, S. Kittner, D. Lloyd-Jones, D. C. Goff, Jr., Y. Hong, R. Adams, G. Friday, K. Furie, P. Gorelick, B. Kissela, J. Marler, J. Meigs, V. Roger, S. Sidney, P. Sorlie, J. Steinberger, S. Wasserthiel-Smoller, M. Wilson, and P. Wolf, "Heart disease and stroke statistics—2006 update: A report from the American Heart Association Statistics Committee and Stroke Statistics Subcommittee," *Circulation*, vol. 113, pp. e85–e151, Feb. 14, 2006.

[2] M. Rubart and D. P. Zipes, "Mechanisms of sudden cardiac death," *J. Clin. Invest.*, vol. 115, pp. 2305–2315, Sep. 2005.

[3] H. V. Huikuri, A. Castellanos, and R. J. Myerburg, "Sudden death due to cardiac arrhythmias," *N. Engl. J. Med.*, vol. 345, pp. 1473–1482, Nov. 2001.

[4] D. P. Zipes, "What have we learned about cardiac arrhythmias?," *Circulation*, vol. 102, pp. 52–57, 2000.

[5] M. Josephson and H. J. J. Wellens, "Implantable defibrillators and sudden cardiac death," *Circulation*, vol. 109, pp. 2685–2691, Jun. 8, 2004.

[6] A. J. Moss, "MADIT-I and MADIT-II," *J. Cardiovasc. Electrophysiol.*, vol. 14, pp. S96–S98, Sep. 2003.

[7] A. I. Mushlin, W. J. Hall, J. Zwanziger, E. Gajary, M. Andrews, R. Marron, K. H. Zou, and A. J. Moss, "The cost-effectiveness of automatic implantable cardiac defibrillators: Results from MADIT. Multi-center automatic defibrillator implantation trial," *Circulation*, vol. 97, pp. 2129–2135, Jun. 1998.

[8] E. Delacretaz and W. G. Stevenson, "Catheter ablation of ventricular tachycardia in patients with coronary heart disease. Part II: Clinical aspects, limitations, and recent developments," *Pacing Clin. Electrophysiol.*, vol. 24, pp. 1403–1411, Sep. 2001.

[9] E. Delacretaz and W. G. Stevenson, "Catheter ablation of ventricular tachycardia in patients with coronary heart disease. Part I: Mapping," *Pacing Clin. Electrophysiol.*, vol. 24, pp. 1261–1277, Aug. 2001.

[10] R. M. Gulrajani, "The forward and inverse problems of electrocardiography," *IEEE Eng. Med. Biol. Mag.*, vol. 17, no. 5, pp. 84–101, Sep./Oct. 1998.

[11] Y. Rudy and R. Plonsey, "A comparison of volume conductor and source geometry effects on body surface and epicardial potentials," *Circ. Res.*, vol. 46, pp. 283–291, 1980.

[12] Y. Serinagaoglu, R. S. MacLeod, B. Yilmaz, and D. H. Brooks, "Multi-electrode venous catheter mapping as a high quality constraint for electrocardiographic inverse solution," *J. Electrocardiol.*, vol. 35, pp. 65–73, 2002.

[13] R. D. Throne and L. G. Olson, "Fusion of body surface potential and body surface Laplacian signals for electrocardiographic imaging," *IEEE Trans. Biomed. Eng.*, vol. 47, no. 4, pp. 452–462, Apr. 2000.

[14] L. K. Cheng, J. M. Bodley, and A. J. Pullan, "Comparison of potential- and activation-based formulations for the inverse problem of electrocardiology," *IEEE Trans. Biomed. Eng.*, vol. 50, no. 1, pp. 11–22, Jan. 2003.

[15] A. A. Armoundas, A. B. Feldman, R. Mukkamala, and R. J. Cohen, "A single equivalent moving dipole model: An efficient approach for localizing sites of origin of ventricular electrical activation," *Ann. Biomed. Eng.*, vol. 31, pp. 564–576, 2003.

[16] A. A. Armoundas, A. B. Feldman, D. A. Sherman, and R. J. Cohen, "Applicability of the single equivalent point dipole model to represent a spatially distributed bio-electrical source," *Med. Biol. Eng. Comput.*, vol. 39, pp. 562–570, Sep. 2001.

[17] A. A. Armoundas, "A novel technique for guiding ablative therapy of cardiac arrhythmias," in *Nuclear Engineering*. Cambridge, MA: MIT Press, 1999.

[18] R. C. Chan, S. B. Johnson, J. B. Seward, and D. L. Packer, "The effect of ablation electrode length and catheter tip to endocardial orientation on radiofrequency lesion size in the canine right atrium," *Pacing Clin. Electrophysiol.*, vol. 25, pp. 4–13, Jan. 2002.

[19] F. Morady, "Radio-frequency ablation as treatment for cardiac arrhythmias," *N. Engl. J. Med.*, vol. 340, pp. 534–544, Feb. 1999.

[20] R. M. Arthur and D. B. Geselowitz, "Effect of inhomogeneities on the apparent location and magnitude of a cardiac current dipole source," *IEEE Trans. Biomed. Eng.*, vol. BME-17, no. 2, pp. 141–146, Apr. 1970.

[21] Y. Fukuoka, T. F. Oostendorp, D. A. Sherman, and A. A. Armoundas, "Applicability of the single equivalent moving dipole model in an infinite homogeneous medium to identify cardiac electrical sources: A computer simulation study in a realistic anatomic geometry torso model," *IEEE Trans. Biomed. Eng.*, vol. 53, no. 12, pp. 2436–2444, Dec. 2006.

[22] E. Frank, "Electric potential produced by two point current sources in a homogenous conducting sphere," *J. Appl. Phys.*, vol. 23, pp. 1225–1228, 1952.

[23] A. A. Armoundas, A. B. Feldman, R. Mukkamala, B. He, T. J. Mullen, P. A. Belk, Y. Z. Lee, and R. J. Cohen, "Statistical accuracy of a moving equivalent dipole method to identify sites of origin of cardiac electrical activation," *IEEE Trans. Biomed. Eng.*, vol. 50, no. 12, pp. 1360–1370, Dec. 2003.

Maya E. Barley was born in London, U.K. She received the B.S. degree in electrical engineering from Rice University, Houston, TX, in 2001, the M.S. degree in electrical engineering and the Ph.D. degree in biomedical and electrical engineering from Massachusetts Institute of Technology (MIT), Cambridge, in 2003 and 2007, respectively.

She is currently a Senior Scientist at Philips Research, Eindhoven, The Netherlands. Her current research interests include imaging systems, algorithms, and devices for catheter ablation therapy planning and guidance.

Antonis A. Armoundas (M'91) was born in Mytilini, Greece. He received the B.S. degree in electrical engineering from the National Technical University of Athens, Athens, Greece, in 1991, the M.S. degree in biomedical engineering from Boston University, Boston, MA, in 1994, and the Ph.D. degree in nuclear engineering from Massachusetts Institute of Technology (MIT), Cambridge, in 1999.

He was a Postdoctoral Fellow with the Division of Molecular Cardiobiology and the Department of Biomedical Engineering, Johns Hopkins University. He is currently an Assistant Professor in Medicine at Harvard Medical School and Massachusetts General Hospital, Charlestown, where he maintains an appointment at MIT. His current research interests include biomedical signal processing, forward and inverse problem solutions, and cellular electrophysiology methods (experimental and modeling).

Richard J. Cohen was born in Brookline, MA. He received the A.B. degree in physics and chemistry from Harvard College, Cambridge, MA, in 1971, the Ph.D. degree in physics from Massachusetts Institute of Technology, Cambridge, in 1976, and the M.D. degree from Harvard Medical School, Boston, MA, in 1976.

Since 1979, he has been with the Massachusetts Institute of Technology, Harvard–MIT Division of Health Sciences and Technology, where he was the Director at the Biomedical Engineering Center and the Cardiovascular Team Leader of the National Space Biomedical Research Institute. He currently holds the Whitaker Professorship in Biomedical Engineering and codirects the Biomedical Enterprise Program. He completed a residency in Internal Medicine at the Peter Bent Brigham Hospital in 1979. His current research interests include the application of physics and engineering to the solution of biomedical problems, in particular in the cardiovascular area.